Supporting Information

Flexible polymer photonic films with embedded microvoids for high-performance passive daytime radiative cooling

Lei Zhou[1,*], Jintao Zhao[1], Haoyun Huang[1], Feng Nan[1,*], Guanghong Zhou[1], Qingdong Ou[2,*]

[1] *Faculty of Mathematics and Physics, Huaiyin Institute of Technology, Huai'an 223003, PR China*

[2] *Department of Materials Science and Engineering, Monash University, Clayton, Victoria 3800, Australia*

*Corresponding author:

E-mail: leizhou@hyit.edu.cn; nf1989@sina.cn; qingdong.ou@monash.edu

This PDF file includes: Methods, Table S1, Figure S1 to S7

Contents:

Section 1. Methods

Sample Preparation: The monodispersed PS microspheres are synthesized following the widely employed quick emulsifier-free emulsion polymerization method.[1] The synthesized PS microspheres were spun in a centrifuge and washed with ethanol 6 times. After the ethanol was completely evaporated, the PS microspheres were dissolved in DI water with a concentration of 10 wt%. To fabricate the PS microsphere templates, the silicon substrate and glass petri dishes are firstly cleaned with isopropylalcohol (IPA), acetone, ethanol, and DI water in successive a way and subsequently dried in an oven. Thereafter, the silicon substrates are ultraviolet-ozone (UVO)-treated for 3 min to improve the surface hydrophilicity. To fabricate the monolayer PS microsphere templates, 1 mL of 10 wt% PS microsphere mixed with 1 mL ethanol solution is drop-casted on the silicon substrate, which is obliquely placed in a petri dish with one end glass substrate constructed on a 1 mm-thick shim, and thermally cured in 70 °C for 3h to evaporate the solvent. To fabricate the 3D close-packed PS microsphere templates, the mixed solution is dispersed on the pre-cleaned silicon substrate and thermally cured in 70 °C for 2 h using self-assembly method.[2,3] Then, the precursors of PDMS premixed with 1/10 cross-linker (Dow Corning Co.) are spin-coated onto the surface of the PS microsphere templates (5000 rpm for 60 s) and transferred into an vacuum oven for the annealing treatment 60°C for 2 h. Subsequently, the PDMS film containing PS microspheres is formed by peeling off from the silicon substrate. Finally, the as-prepared structured PDMS film is transferred into an oven for the annealing treatment (180 °C, 3 h) to remove PS

microsphere array and thereafter the 3D microvoid arrays-structured PDMS radiator film is obtained.

***Characterization*:** The SEM images of various polymer films were characterized by SEM (FE-SEM, Quanta 250FEG). The total reflection spectra in visible region are measured by a spectrophotometer (Lambda750S, PerkinElmer, Inc.) with an integrating sphere. The reflection (R) and transmission (T) spectra in MIR region are characterized by a Fourier transform infrared spectrometer (FTIR, IRAffinity, Shimadzu) with an infrared integrating sphere. The absorptivity spectra (A) are subsequently calculated using the equation of A = 1-R-T. IR pictures are taken by a portable thermal imaging camera (T650sc, FLIR systems). The Yong's modulus of the films is measured by using material testing machine (Instron 5967).

Optical Simulation: The FDTD method is employed to perform the near-field profile and absorptivity/emissivity spectra of PDMS radiator films. In the simulation, the real and imaginary parts of the refractive index of PDMS are determined according to the experimental data (Figure S1), and a normal plane wave source is incident along *z* direction, using perfect matched boundary (PML) layers in *z* dimensions and periodic boundary conditions in *x* and *y* directions, where the microvoid arrays are arranged as the close-packed face-centered-cubic (FCC) crystals structure in the range of 4 periods with various measured diameters. The thicknesses of both structural films (D = 1 μm and D = 5 μm) are set as 15 μm and 60 μm, and the *z*-axis monitoring range of frequency-domain field and power monitors are set as 8 μm and 40 μm to record the near-field electric field distributions, respectively. The

absorptivity of the radiator is equal to A = 1-R-T. The cross-section near-field Poynting vector distributions of the radiator are calculated using the FDTD method associated with in-house generated codes. The net cooling power is calculated using the measured conditions and detailed in Supporting Information Section 5.

Section 2. Summary of material composition, structures design and cooling performance of daytime passive radiative coolers.

Table S1. Summary of radiative coolers at daytime reported in the literature in comparison with this work. [4-13]

Ref.	Material	Testing time	Peak solar intensity (W/m^2)	Maximum Temperature drop (℃)
[4]	$P(VDF\text{-}HFP)_{HP}$	12:00-13:00	890	6
[5]	Delignificated and mechanically pressed wood	11:00-14:00	700	4
[6]	$SiO_2/Si_3N_4/Al_2O_3$/Ag/Silica	11:00-16:00	872	8.2
[7]	SiO_2/HfO_2/metal	13:00-14:00	890	4.9
[8]	PDMS/Silica/silver	12:00-14:00	NA	8.2
[9]	PVDF/TEOS/Silica	12:00-16:00	1000	6
[10]	Silica-polymer/Ag hybrid metamaterial	12:30-15:00	710	10.6
[11]	SiO_2-coated AAO/Ag	11:30-15:30	610	6.1
[13]	PMMA film with a micropore array and random nanopores	12:00-14:00	900	6.0
This work	PDMS (3D inverse-opal-like structure)	11:00-15:00	870	5.8

Section 3. Calculated absorptivity/emissivity spectra of the microvoids-structured PDMS radiators with various diameters.

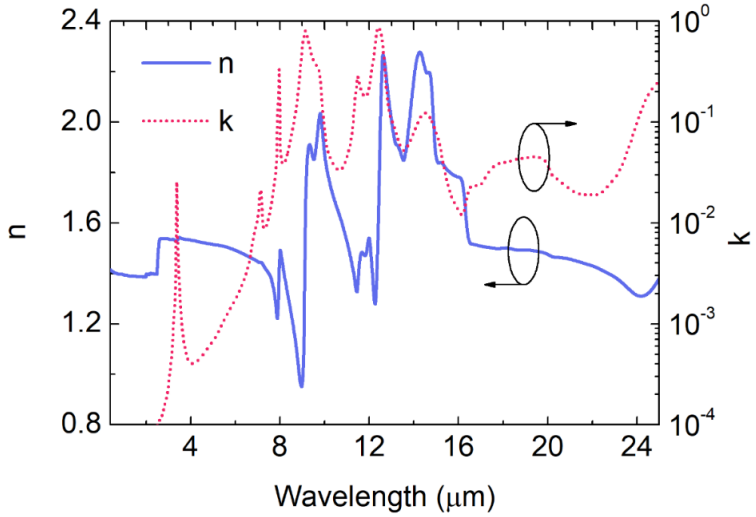

Figure S1. The real and imaginary parts of the refractive index of PDMS, which are extracted from our FTIR experimental measurement following the process outlined by Verleur [10].

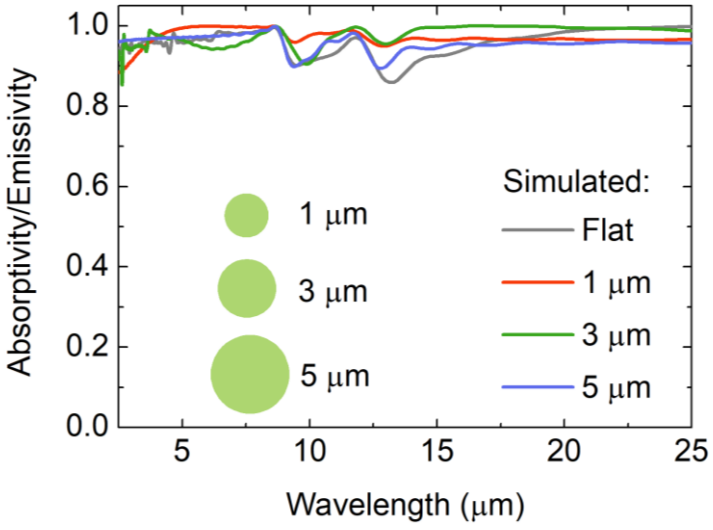

Figure S2. Calculated absorptivity/emissivity spectra of the microvoids-structured

PDMS radiators within the MIR wavelength region with various diameters. The thickness of the film is set as 300 μm.

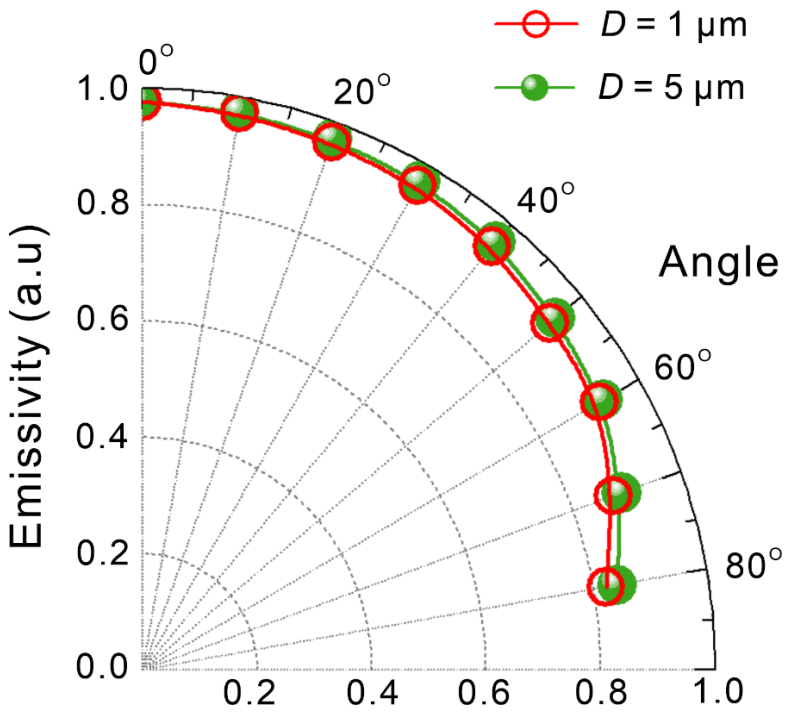

Figure S3. The simulated distribution of the average absorbtivity/emissivity across the atmospheric window of the structural films with bulilt-in microvoids at different polarization angles.

Section 4. Passive radiative cooling performance measurement of the planar PDMS radiator film.

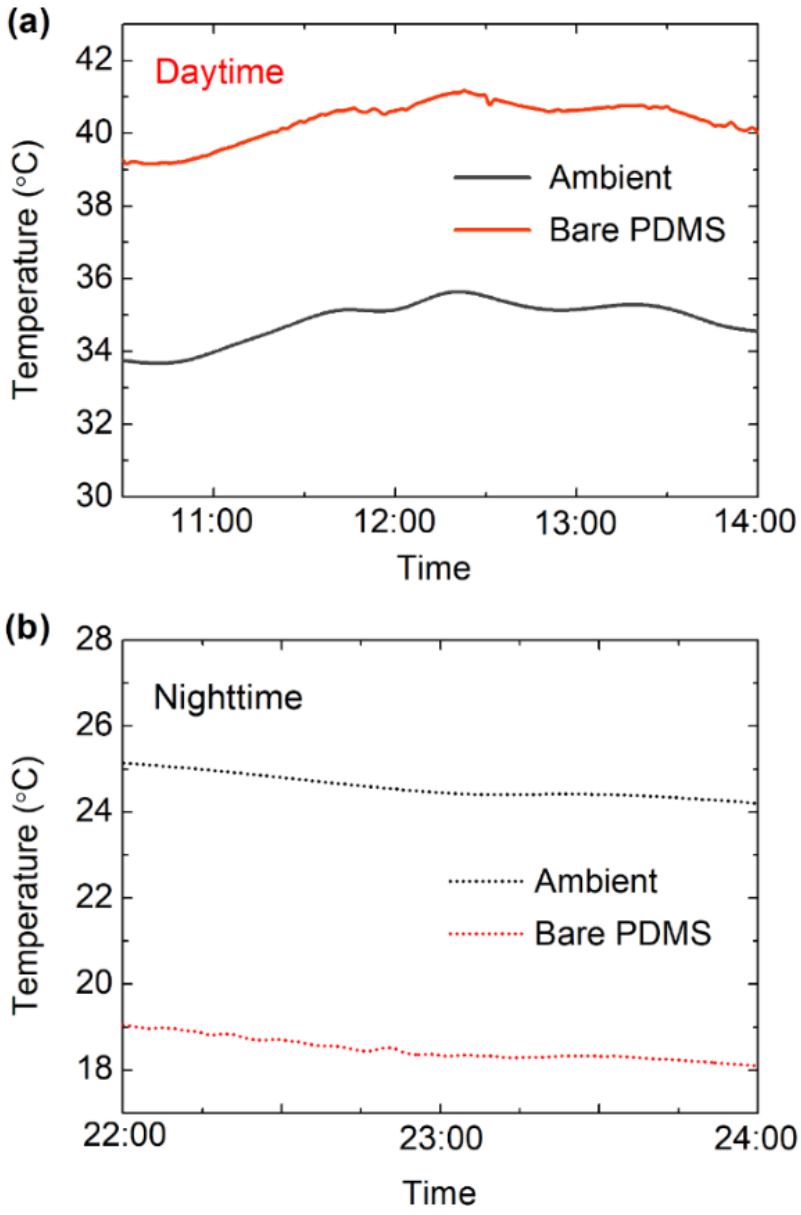

Figure S4. Measured temperature difference achieved for the planar PDMS radiator film at (a) daytime, and (b) nighttime (01/08/2020 to 02/08/2020).

As depicted in Figure S3, although the planar PDMS radiator film achieves satisfying cooling performance at nighttime (~ 6-7 °C), its temperature is ~ 5-6 °C higher than the ambient at noon, since the sunlight is not efficiently scattered or reflected by the flat PDMS film. This capability stems from intrinsic property of the PDMS material, which has negligible extinction coefficient in the solar irradiation spectrum region and relatively strong extinction ability in the MIR range. Namely, the planar PDMS film is suitable for passive nighttime radiative cooling, but not for daytime radiative cooling.

Section 5. Principle of radiative cooling and near-field optical simulation

To analyze the cooling efficiency, the net cooling power of our proposed radiator film is calculated, considering a radiator at temperature T_{sample} corresponds to ambient air temperature T_{amb}. Taking into all the heat exchange progress, the net cooling power of a daytime radiative cooler can be expressed as [11,12]

$$P_{net}(T_{sample}) = P_{rad}(T_{sample}) - P_{atm} - P_{sun} - P_{cond+conv} \quad (1)$$

where

$$P_{rad}(T_{sample}) = \int d\Omega cos\theta \int_0^\infty d\lambda I_{BB}\left(T_{sample}, \lambda\right) \varepsilon(\lambda, \theta) \quad (2)$$

is the outward radiation power of the radiator,

$$P_{atm}(T_{amb}) = \int d\Omega cos\theta \int_0^\infty d\lambda I_{BB}(T_{amb}, \lambda)\, \varepsilon(\lambda, \theta)\varepsilon_{atm}(\lambda, \theta) \quad (3)$$

is the absorbed power due to the incident atmospheric thermal radiation,

$$P_{sun}(T_{sample}) = \int_0^\infty d\lambda\, \varepsilon(\lambda, \theta_{sun}) I_{AM1.5}(\lambda) \quad (4)$$

is the incident solar irradiation power absorbed by the radiator, and

$$P_{cond+conv} = \left(T_{sample}, T_{amb}\right) = h_c(T_{amb} - T_{sample}) \quad (5)$$

is the power density of nonradiative heat exchange due to convection and conduction. Here,

$$\int d\Omega = 2\pi \int_0^{\frac{\pi}{2}} d\theta sin\theta \quad (6)$$

is the angular integral over hemisphere.

$$I_{BB}\left(T_{sample}, \lambda\right) = 2hc^2/\lambda^5(e^{\frac{hc}{\lambda k T_{sample}}} - 1) \quad (7)$$

is the spectral radiance of a blackbody at T_{sample}, where h, c, k and λ represent

the Planck's constant, the speed of light, the Boltzmann constant, and the wavelength, respectively. $\varepsilon(\lambda,\theta)$ represents the directional emissivity of the radiator at the wavelength of λ, which equal to its absorptivity according to Kirchhoff's law, $I_{AM1.5}(\lambda)$ denotes the AM1.5 solar illumination with total solar irradiance of ~ 1 KW· m^{-2}, and h_c is the combined conduction and convection heat transfer coefficient.

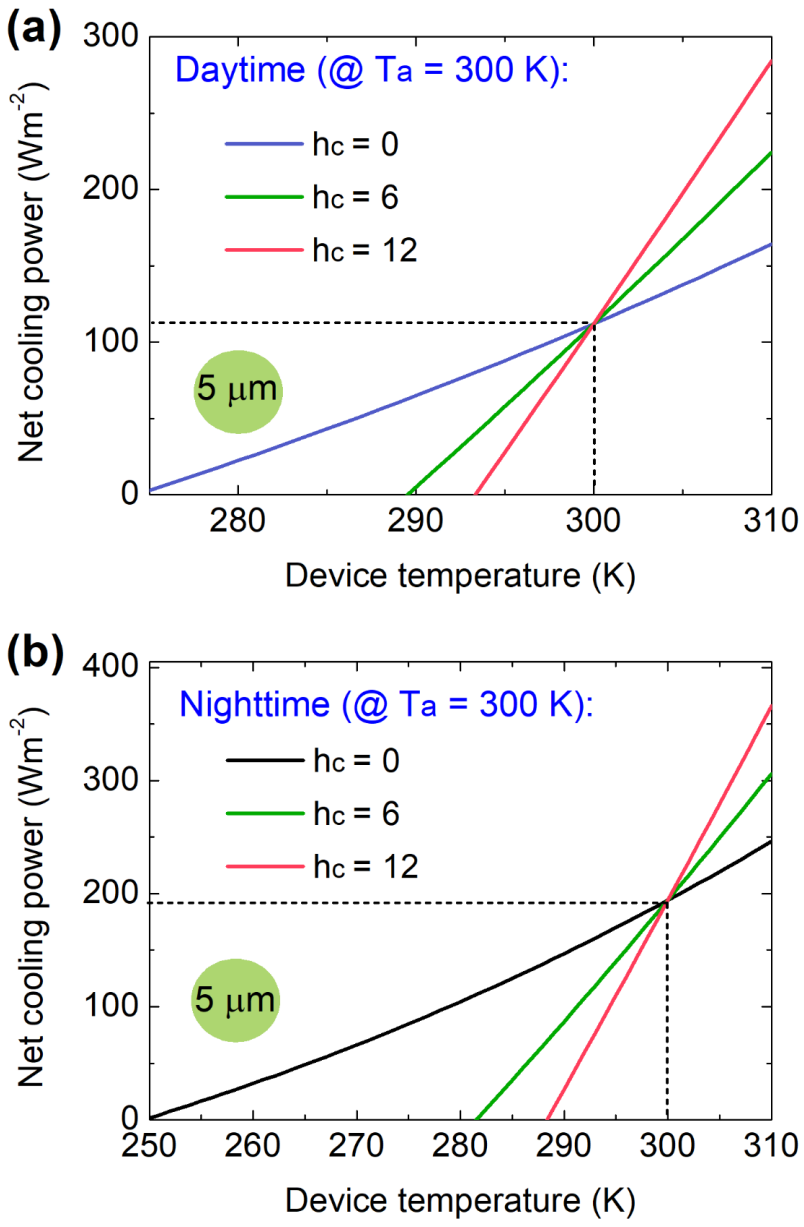

Figure S5. (a) Daytime and (b) nighttime net cooling power as a function of device

surface temperature of the structural film (D = 5 μm). Here, T_a denotes the ambient temperature.

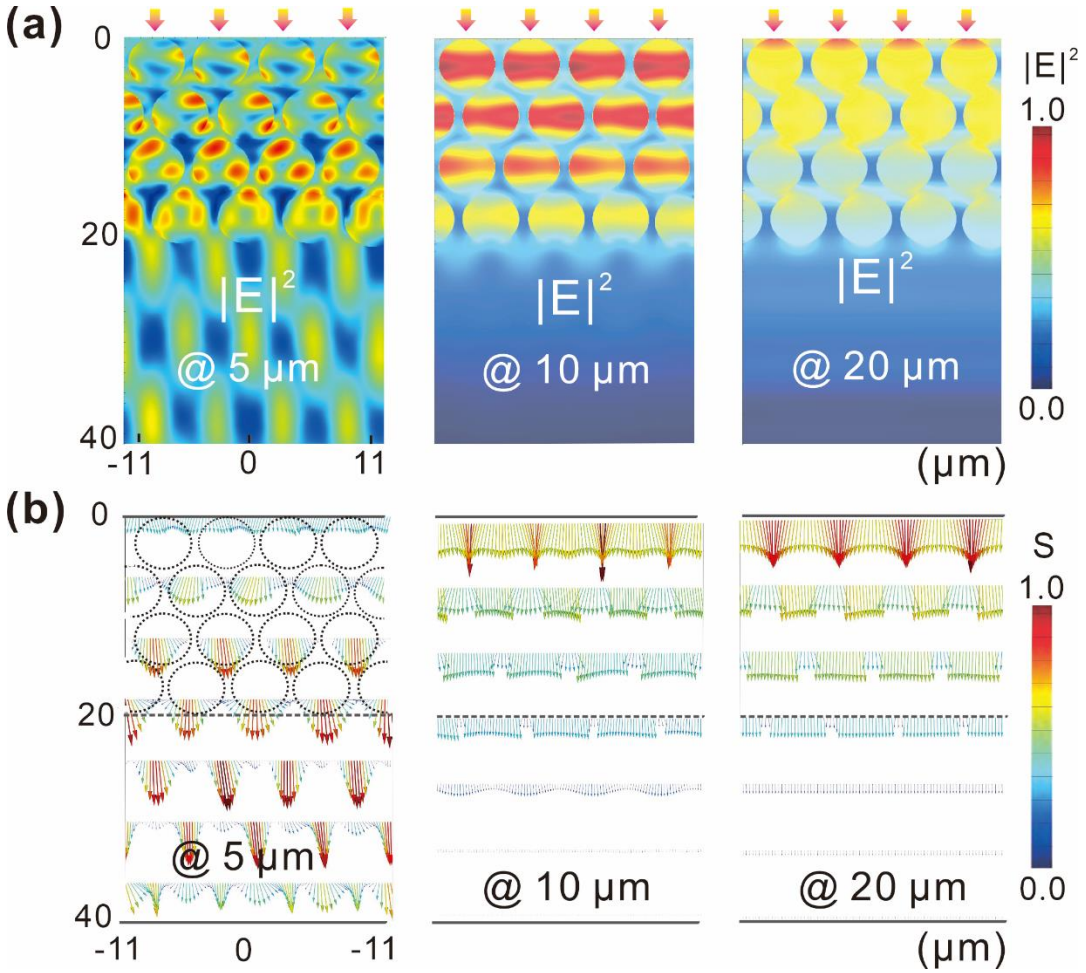

Figure S6. Simulated distributions of (a) the electric field profiles and (b) the corresponding time-average energy flux distributions for the structural radiator (D = 5 μm) at three different wavelengths.

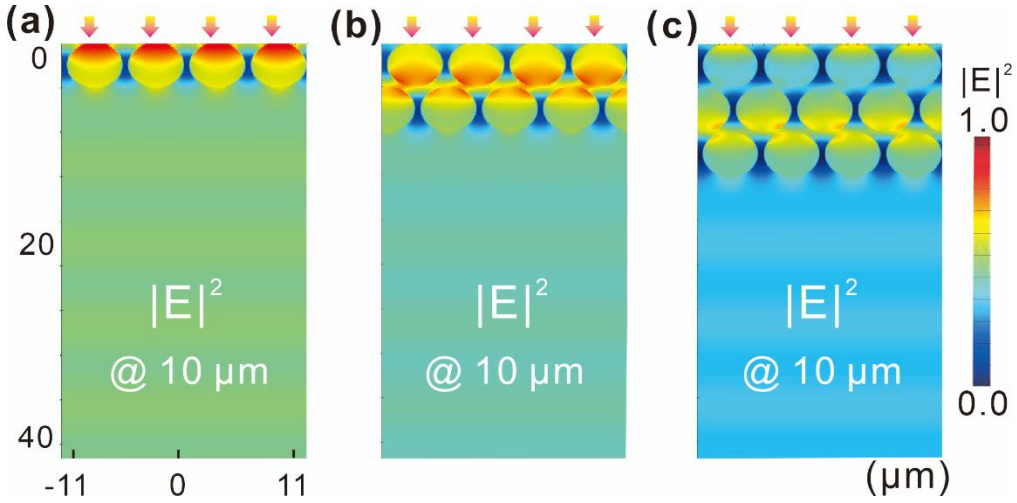

Figure S7. Simulated distributions of the electric field profiles of the structured polymer radiators with a) monolayer, b) double-layers and c) three-layers microvoids, respectively.

REFERENCES

(1) Du, X.; He, J. Facile Size- controllable Syntheses of Highly Monodisperse Polystyrene Nano- and Microspheres by Polyvinylpyrrolidone- mediated Emulsifier- free Emulsion Polymerization. *J. Appl. Polym. Sci.* **2008**, *108*, 1755-1760.

(2) Wang, D.; Caruso, F. Fabrication of Polyaniline Inverse Opals via Templating Ordered Colloidal Assemblies. *Adv. Mater.* **2001**, *13*, 350-354.

(3) Ye, Y. H.; Badilescu, S.; Truong, V. V.; Rochon, P.; Natansohn, A. Self-assembly of Colloidal Spheres on Patterned Substrates. *Appl. Phys. Lett.* **2001**, *79*, 872-874.

(4) Mandal, J.; Fu, Y.; Overvig, A. C.; Jia, M.; Sun, K.; Shi, N. N.; Zhou, H.; Xiao, X.; Yu, N.; Yang, Y. Hierarchically Porous Polymer Coatings for Highly Efficient Passive Daytime Radiative Cooling. *Science* **2018**, *362*, 315-319.

(5) Li, T.; Zhai, Y.; He, S.; Gan, W.; Wei, Z.; Heidarinejad, M.; Dalgo, D.; Mi, R.; Zhao, X.; Song, J.; Dai, J.; Chen, C.; Aili, A.; Vellore, A.; Martini, A.; Yang, R.; Srebric, J.; Yin,X.; Hu, L. A Radiative Cooling Structural Material. *Science* **2019**, *364*, 760-763.

(6) Chae, D.; Kim, M.; Jung, P. H.; Son, S.; Seo, J.; Liu, Y.; Lee, B. J.; Lee, H. Spectrally Selective Inorganic-based Multilayer Emitter for Daytime Radiative Cooling. *ACS Appl. Mater. Interfaces* **2020**, *12*, 8073-8081.

(7) Raman, A. P.; Abou Anoma, M.; Zhu, L.; Rephaeli, E.; Fan, S. Passive Radiative Cooling below Ambient Air Temperature under Direct Sunlight. *Nature* **2014**, *515*, 540-544.

(8) Goldstein, E. A.; Raman, A. P.; Fan, S. Sub-ambient Non-evaporative Fluid Cooling with the Sky. *Nat. Energy* **2017**, *2*, 1-7.

(9) Wang, X.; Liu, X.; Li, Z.; Zhang, H.; Yang, Z.; Zhou, H.; Fan, T. Scalable Flexible Hybrid Membranes with Photonic Structures for Daytime Radiative Cooling. *Adv. Fun. Mater.* **2020**, *30*, 1907562.

(10) Zhao, D.; Aili, A.; Zhai, Y.; Lu, J.; Kidd, D.; Tan, G.; Yin, X.; Yang, R. Subambient Cooling of Water: Toward Real-world Applications of Daytime Radiative Cooling. *Joule* **2019**, *3*, 111-123.

(11) Lee, D.; Go, M.; Son, S.; Kim, M.; Badloe, T.; Lee, H.; Kim, J.; Rho, J.

Sub-ambient Daytime Radiative Cooling by Silica-coated Porous Anodic Aluminum Oxide. *Nano Energy* **2021**, *79*, 105426.

(12) Wang, T.; Wu, Y.; Shi, L.; Hu, X.; Chen, M.; Wu, L. A Structural Polymer for Highly Efficient All-day Passive Radiative Cooling. *Nat. Commun.* **2021**, *12*, 1-11.

(13) Verleur, H. W. Determination of Optical Constants from Reflectance or Transmittance Measurements on Bulk Crystals or Thin Films. *J. Opt. Soc. Am.* **1968**, *58*, 1356-1364.

(14) Hossain, M. M.; Gu, M. Radiative Cooling: Principles, Progress, and Potentials. *Adv. Sci.* **2016**, *3* 1500360.

(15) Raman, A. P.; Abou Anoma, M.; Zhu, L.; Rephaeli, E.; Fan, S. Passive Radiative Cooling Below Ambient Air Temperature under Direct Sunlight. *Nature* **2014**, *515*, 540-544.